Control of vortex pinning in YBCO thin films by incorporating APCs through surface modified target approach

Alok K. Jha* and Kaname Matsumoto

Department of Materials Science and Engineering, Kyushu Institute of Technology, Tobata-ku, Kitakyushu-shi 804-8550, JAPAN

***E-mail: akjha@post.matsc.kyutech.ac.jp**

Abstract:

The transport of electrical currents in superconductors with much higher efficiency and without any dissipation is considered as the 'energy superhighway'. After the discovery of $YBa_2Cu_3O_{7-\delta}$ (YBCO), a high temperature superconductor (HTS), the prospect of using superconducting materials in practical technological applications became very prominent. With much higher T_c (~ 92 K) than conventional low temperature superconductors (LTS), YBCO was considered very promising due to cheaper cooling requirements. The evolution of critical current density (J_c), however, took long time for the material to become useful in practical applications. This was achieved through continuous modification of the processing parameters, deposition of highly oriented thin films on single crystal and buffered metallic substrates and use of artificial pinning centers (APCs) for strong pinning of quantized magnetic vortices.

Pulsed laser deposition (PLD) technique is one of the most common and highly efficient techniques for depositing highly oriented YBCO thin films on single crystal and buffered metallic substrates. Using PLD technique, APCs are incorporated into YBCO thin films by many methods which include premixed target method, alternating target method and surface modified target method.

In this chapter, the use of surface modified target method to introduce different kinds of

APCs into YBCO thin films is presented. These APCs are effective in improving the vortex pinning properties of YBCO thin films for different range of applied magnetic field and its orientation depending upon their geometry and density.

1. $YBa_2Cu_3O_{7-\delta}$: A promising high temperature superconductor

$YBa_2Cu_3O_{7-\delta}$ (YBCO) was discovered as the first superconductor which exhibited superconducting transition above the liquid nitrogen temperature (77 K) [1]. The discovery of YBCO accelerated the search for higher transition temperature (T_c) materials leading subsequently to the discovery of other superconductors such as $Bi_2Sr_2Ca_2Cu_3O_{10+\delta}$ [2] and $HgBa_2Ca_2Cu_3O_{8+\delta}$ [3] which exhibited higher T_c than YBCO. YBCO, however, has couple of advantages over other cuprate superconductors which include easier synthesis methods and much larger critical current density (J_c) at 77 K. J_c is the most relevant parameter of a superconductor which decides the ability of a superconductor to be used in practical applications [4-6]. The electronic structure, critical temperature and the mechanism of vortex pinning determine J_c in any superconductor. In addition, the irreversibility field (H_{irr}) for YBCO is also much larger than for any other cuprate superconductor at 77 K. H_{irr} is a very important parameter which determines the upper limit of J_c in a superconductor. The irreversibility line marks the separation between the solid-liquid phases of the vortex matter and much effort has been made to shift this line towards higher *H-T* regime by artificial pinning center technology [4, 6-8].

2. The evolution of critical current density of YBCO superconductor over time:

Polycrystalline bulk samples of YBCO were observed to have very low J_c (~ 10^2 A/cm^2) despite exhibiting high T_c (~ 92 K), and relatively large $\mu_0 H_{irr}$ (~ 7 T at 77 K). The reason for low J_c in polycrystalline samples was ascribed to small coherence length

of YBCO, which limits the percolation of electrical current across grain boundaries [9]. Additionally, the anisotropic character of its J_c (which is higher along the *ab*-plane than along the *c*-axis) is also partially responsible for low J_c in the polycrystalline samples. The alignment of the grains was improved by melt-texturing-growth (MTG) method [10, 11] which resulted in much higher J_c (~ 10^4 A/cm^2). However, still the value of J_c was too low for the possibility of any practical use of YBCO.

Thanks to the continuous efforts from researchers across the world, it became possible to make thin films of YBCO on single crystal substrates such as $SrTiO_3$, Al_2O_3, MgO, etc. [12]. Highly *c*-axis oriented thin films of YBCO on single crystal substrates exhibited $J_c > 10^6$ A/cm^2 (at 77 K) which was much higher than that for MTG YBCO samples. The fabrication and processing techniques developed over the years resulted in the current carrying capability of YBCO significantly enhanced. Through many deposition techniques such as pulsed laser deposition (PLD) [13], chemical solution deposition (CSD) [14] and metal organic chemical vapor deposition (MOCVD) [15], it became possible to prepare highly *c*-axis oriented YBCO thin films which exhibited high J_c of 1–5 MA/cm^2 at 77 K, self-field [16, 17].

3. Critical current density under applied magnetic field and pinning of vortices by APCs in YBCO films:

A type-II superconductor, when subjected to an applied magnetic field (H), remains in different states depending upon the strength of H [18]. It has two critical magnetic fields namely: (i) lower critical field (H_{c1}) and (ii) upper critical field (H_{c2}). When $H < H_{c1}$, the superconductor exhibits perfect diamagnetism by expelling the magnetic field completely and is said to be in the Meissner state. When $H_{c1} < H < H_{c2}$, the magnetic field penetrates the superconductor in a form of small “tubes” (vortices), each with

quantized flux $\Phi_0 = h/(2e)$. The number and thus density of the vortices continue to increase until the applied magnetic field reaches a value equal to H_{c2}. This state of a type-II superconductor is called mixed state or vortex state. When $H > H_{c2}$, the superconductor goes into the normal state.

When a type-II superconductor (such as YBCO) is in its mixed state and an electrical current is flown across it, the vortices experience a Lorentz force, whose density (F_L) is given by the vector product of the current density J and applied magnetic field $\mu_0 H$. This Lorentz force pushes the vortices in a direction perpendicular to both the electrical current and the applied magnetic field. There are, however, some microscopic defects that are generated naturally during the growth of the superconducting samples which prevent the motion of the vortices under the influence of Lorentz force. The vortices are thus pinned by these defects and these defects, therefore, are termed as pinning centers. The force which resists the motion of vortices under the influence of the Lorentz force is called pinning force whose magnitude per unit volume is called pinning force density (F_p). The vortices remain stationary, as long as the pinning force is greater than the Lorentz force. When the Lorentz force on the vortices exceeds the pinning force, they start moving across the superconducting sample. If the vortices move with a velocity v a finite electric field $E = \mu_0 H \times v$ would be generated. Since, current and the generated electric field have the same direction, a finite power would be dissipated in the system and the ability of the superconductor to sustain dissipation-free current flow would be lost. The vortices in YBCO thin films are pinned by some naturally occurring defects (which are formed during the growth of the film) such as dislocations, grain boundaries, twin boundaries, oxygen vacancies, *etc*. The strength of these naturally occurring defects, however, is not enough to counter thermal fluctuations and their densities are

not sufficient to maintain large J_c at high magnetic fields [6, 19, 20].

It, therefore, became imperative to look for alternative ways which can be efficient for pinning the vortices even at high applied magnetic fields. This arose the need for artificial pinning centers (APCs) and their introduction turned out to be very effective for the immobilization of the vortices even at high applied magnetic fields leading to enhanced J_c of YBCO thin films for wide range of applied magnetic field. The introduction of APCs into YBCO films have been conducted through various methods which include heavy ion irradiation [21], addition and/or substitution of rare-earth atoms [22, 23] or incorporation of secondary phase nanoinclusions into the YBCO film matrix [24-34]. Enhancement of vortex pinning properties of YBCO films through incorporation of secondary phase nanoinclusions has recently been extensively studied. The nanoinclusions of several materials such as Y_2BaCuO_5 [24, 25], Y_2O_3 [26], $BaZrO_3$ [27, 28], $BaSnO_3$ [29, 30], $BaIrO_3$ [31], YBa_2NbO_6 [32, 33], YBa_2TaO_6 [34] have been successfully introduced into YBCO film matrix by using PLD technique, which led to the enhancement of J_c of YBCO thin films over a wide range of applied magnetic field.

4. Methods to introduce APCs in YBCO films through PLD technique:

In PLD technique, a laser pulse is focused onto the surface of a target (the material whose thin film has to be prepared) inside a vacuum chamber. Above a certain threshold energy density, the target material is sputtered and the ejected species forms a luminous ablation plume. The sputtered material is directed towards a substrate where it condenses to form a film. In the case of YBCO films, the nanoinclusions of secondary phase materials are usually introduced by two methods: (i) by mixing the secondary phase material with YBCO and making a premixed target and (ii) using two different targets of YBCO and secondary phase material and ablate them alternatively during the

deposition process. The advantage of using premixed target is that if offers precise control over the volume percentage of the secondary phase into the YBCO film matrix. However, the secondary phase material needs to be non-reactive with YBCO in the sintering temperature range of 920-950 ℃ which is usually higher than the deposition temperature of the films (800-830 ℃). The alternating target approach also provides precise control of the concentration of the secondary phase in YBCO films and also removes the possibility of any chemical reaction between YBCO and the secondary phase in the ablation target, but this process is time consuming.

5. The surface modified target method:

In order to introduce nanoscale secondary phases into YBCO thin films using PLD technique, a novel method is adopted in which the surface of the ablation target is modified and that is why this method is named as surface modified target method. In this method, a thin sectored or rectangular shaped piece of secondary phase material is attached on the top of YBCO target using silver paste [35, 36]. The schematic diagram of this method is shown in figure 1. The main advantage of this approach is that the secondary phase material can be continuously introduced into YBCO film using a single target in which YBCO portion and secondary phase material portion are physically separate. Also, the concentration of the secondary phase can be varied just by changing the size of the sectored/rectangular shaped piece of secondary phase material while keeping the YBCO target the same. Mele *et al.* [37] have reported the observation of $BaZrO_3$ nanocolumns within YBCO film matrix for which YBCO+YSZ (yttria stabilized zircornia) surface modified target was used.

It is quite interesting to compare surface modified target method with premixed target method from the point of view of growth mechanism of different phases in a thin film.

In the mixed target method, the adatoms or molecules of both the species (YBCO and the secondary phase) are continuously supplied and the supersaturation of YBCO is higher than that of the secondary phase material (as the mixed target consists of YBCO phase in larger proportion than the secondary phase material). In the surface modified target method, however, the adatoms or molecules of different species are transported to the substrate surface in an alternative and periodic manner and for this reason the supersaturation of YBCO and the secondary phase may be considered as the same. In spite of the different scenario of supersaturation in these two methods, the microstructure of the final films reveals similar features: formation of nanocolumns or nanoparticles of secondary phases within YBCO matrix. The formation of yttria nanoparticles has been observed in an earlier report [26] in which alternating target method was employed and in that case, the formation of semi-coherent interfaces between the phases can be held responsible for such nanoparticle formation. Using surface modified target method, gold was introduced in the form of nanorods with widely varying diameters within $GdBa_2Cu_3O_{7-\delta}$ (GdBCO) film matrix [38]. According to this report, a gold sheet of 25 mm length and 2 mm width was attached to the top surface of the GdBCO target for supply of gold inside GdBCO film matrix. However, the driving force for the formation of gold nanorods within the GdBCO film matrix is not understood.

6. The realization of nanoscale secondary phase inclusions with different geometries into YBCO matrix:

6.1 YBCO films consisting of nanoparticles of secondary phases (3D APCs):

The layered structured of YBCO gives rise to an intrinsic anisotropy in its properties which is reflected in its J_c as well [39-41]. In general, at a given magnetic field; J_c for H

parallel the *ab*-plane is higher than for *H* parallel the *c*-axis. In order to reduce this anisotropy (making J_c uniform for all the orientations of applied magnetic field), different kinds of APCs are studied which include spherical nanoparticles and columnar nanorods of different secondary phase materials.

In an ideal situation, the nanoparticles of secondary phase materials pin the vortices with the same strength irrespective of the applied magnetic field orientation. Although, the vortex cross-section changes with the orientation of the applied magnetic field but the interacting volume of the vortex and a spherical nanoparticles does not change significantly and the pinning strength of such APCs does not change much with the orientation of applied magnetic field. For this reason, the nanoparticles of secondary phases are called 3D APCs. Nanocolumnar structures, on the other hand, are called 1D APCs which pin segments of the vortices depending upon the orientation of the applied magnetic field. As the applied field is tilted from the 1D APC orientation, the pinned segment of the vortex decreases and this leads to reduced pinning efficiency of 1D APCs. 3D APCs (nanoparticles), therefore, are preferred over 1D APCs (nanocolumns) for many applications where reduced anisotropy is desired.

The use of spherical nanoparticles or so called 3D APCs was reported by Haugan *et al.* [25] and Varanasi *et al.* [35] in which Y_2BaCuO_5 (Y211) nanoparticles were found to improve the in-field J_c of YBCO thin films. However, the angular dependent J_c study was not conducted in their reports. In these reports, however, the Y211 nanoparticles were introduced into YBCO thin film by alternating target method. Similarly, Y_2O_3 nanoparticles were also introduced as 3D APCs into YBCO thin films by alternating target method and they were effective in reducing the J_c anisotropy of YBCO thin films as observed in the angular dependent J_c study [42]. Later, both Y_2O_3 and Y211

nanoparticles were introduced into YBCO thin films independently by surface modified target method. Mele *et al.* [36] used the surface modified target method for the incorporation of Y_2O_3 nanoparticles into YBCO thin films. Although, the microstructure clearly revealed the formation of Y_2O_3 nanoparticles within YBCO film matrix, the anisotropy in J_c could not be improved significantly. For higher concentration of Y_2O_3 into YBCO thin films, they were observed in the form of nanorods as well [43].

In a recent work, the incorporation of Y211 nanoparticles into YBCO films, through surface modified target method, has been reported [24]. The concentration of Y211 nanoparticles were varied systematically by changing the size of the Y211 surface modified piece on top of the YBCO target. Figure 2 shows the microstructure of the YBCO thin films with varying concentration of Y211 nanoparticles. These Y211 nanoparticles not only enhanced the in-field J_c of YBCO thin films but also shifted the irreversibility line toward higher *H*-*T* regime. Angular dependent J_c studies for YBCO thin films with different concentrations of Y211 nanoparticles were conducted and it was found that these Y211 nanoparticles are very effective in reducing the J_c anisotropy of YBCO thin films. Figure 3 shows the angular dependent J_c curves for YBCO thin films, with varying concentrations of Y211 nanoparticles, measured at different magnetic fields at 65 K. These Y211 nanoparticles resulted in almost isotropic J_c of YBCO thin films barring only a narrow angular range near the *ab*-plane. This feature was further analysed by existing theoretical models and it was suggested that in this narrow angular range of applied magnetic field, there is a cross-over from nanoparticle pinning to *ab*-plane pinning which results from the linear defects (planar defects such as stacking faults) aligned along the *ab*-plane. Figure 4 shows the schematic diagram of

such a situation where pinning due to nanoparticles and linear disorders along the *ab*-plane dominate for different angular range of applied magnetic field.

6.2 YBCO films consisting of nanocolumns of secondary phases (1D APCs):

Columnar disorders along the *c*-axis of YBCO films are generated through heavy-ion irradiation or formation of self-assembled nanocolumns of some secondary phase materials such as $BaZrO_3$ (BZO), $BaSnO_3$ (BSO), $BaHfO_3$ (BHO), YBa_2NbO_6 (YBNO), YBa_2TaO_6 (YBTO) *etc.* The pinning efficiency of these columnar nanostructures (1D APCs) is very high which results in significantly enhanced in-field J_c of YBCO films. The efficiency of these 1D APCs, however, is limited for a small angular range where the applied field is oriented along the *c*-axis or is slightly inclined with respect to the *c*-axis. For this reason, the angular dependent J_c of the YBCO thin films containing 1D APCs exhibits a peak when the applied field is along the *c*-axis.

The use of surface modified target to introduce 1D APCs into YBCO films started more than a decade ago when Varanasi *et al.* successfully introduced BSO nanostructures into YBCO thin films [44]. The incorporation of BSO nanostructures into YBCO thin films resulted in enhanced in-field J_c of YBCO thin films. However, the microstructure of the nanocomposite film was not studied in detail and it was assumed on the basis of planar view of the transmission electron microscope (TEM) image that the BSO nanostructures are organized in the form of nanoparticles inside YBCO film matrix. But, in subsequent studies [30, 45], the cross-sectional view of the YBCO+BSO nanocomposite film was observed which revealed columnar structures and self-assembly of BSO phase in the form of nanocolumns inside YBCO film matrix was confirmed. Figure 5 shows the cross-sectional TEM image of YBCO+BSO nanocomposite film deposited by surface modified target method in which columnar nanostructures can be clearly observed. The

efficiency of these BSO nanocolumns can be seen in figure 6 in which significant enhancement in the in-field J_c of the nanocomposite films can be observed.

Apart from BSO, BZO and YBNO nanocolumns have also been successfully incorporated into YBCO film matrix by surface modified target method. Mele *et al.* used yttria-stabilized-zirconia (YSZ) as a surface modified piece on top of YBCO target which led to the formation of BZO nanocolumns inside YBCO film matrix [46]. These columnar APCs resulted in enhanced in-field J_c of the YBCO+YSZ films. Figure 7 shows the cross-sectional TEM image of the YBCO+YSZ films in which the formation of 1D APCs can be clearly observed. Significant enhancement in the in-field J_c can be observed in figure 8 which is reflected in the much higher F_p values for the nanocomposite film (inset of figure 8). In another work, surface modified target method was used to incorporate YBNO nanocolumns into YBCO film matrix [47]. In this work, the concentration of the YBNO phase inside YBCO thin film was controlled by controlling the target rotation speed. Figure 9 shows the cross-sectional TEM image of YBCO+YBNO nanocomposite films in which not only formation of columnar YBNO nanostructures can be seen but also the variation in the density of YBNO nanocolumns can be observed. The incorporation of YBNO nanostructures inside YBCO films resulted in enhanced in-field J_c of the YBCO thin films which is shown in figure 10. Figure 10 (c) reveals the J_c peak for H // c-axis for YBCO+YBNO nanocomposite thin films in the angular dependent J_c measurement.

6.3 YBCO films consisting of both nanoparticles and nanocolumns of secondary phases (1D + 3D APCs):

Both columnar nanostructures (1D APCs) and spherical nanoparticles (3D APCs) can be introduced into YBCO films and both can be effective in enhancing the in-field J_c.

However, they have completely different effect on the J_c anisotropy. 1D APCs provide strong pinning but their efficiency is limited for a narrow angular range when applied magnetic field is parallel to the orientation of the columnar nanostructures. 3D nanoparticles, on the other hand, are less strong pinning centres but they provide isotropic pinning which is very much desired for many applications. In order to combine these different characteristics of both kind of APCs, YBCO thin films with both kinds of APCs, called hybrid APCs, were prepared. Surface modified target method has also been used to introduce hybrid APCs which turned out to be effective in enhancing the J_c as well as in reducing the J_c anisotropy.

The use of surface modified target for simultaneous incorporation of both 1D and 3D APCs into YBCO thin films was reported by Mele *et al.* who successfully introduced BZO nanocolumns and Y_2O_3 nanoparticles together into YBCO thin films [48, 49]. This combination, however, could not improve the anisotropy of the YBCO film as compared to the YBCO thin film with single APCs (either BZO or Y_2O_3). This technique of using hybrid APCs was later attempted successfully to introduce BSO nanocolumns together with Y_2O_3 (YO) nanoparticles into YBCO thin films by means of surface modified target method [50, 51]. These hybrid APCs were very effective in improving the in-field J_c of YBCO films as well as reducing its angular anisotropy. Figure 11 shows the cross-sectional TEM image of YBCO+BSO3% and YBCO+BSO3%+Y_2O_3 nanocomposite thin films in which formation of only columnar structures in YBCO+BSO thin film and that of both nanocolumns and nanoparticles in YBCO+BSO+Y_2O_3 thin film can be clearly observed. Figure 12 shows the angular dependent J_c measurement conducted at 77 K, 1 T and 65 K, 3 T for pristine YBCO, YBCO+BSO, and YBCO+BSO+Y_2O_3 thin films. It can be clearly observed that the

samples consisting of hybrid APCs exhibit superior in-field J_c not only along the *c*-axis but for entire range of angular orientation of applied magnetic field.

In another work, the successful incorporation of a different combination of nanocolumns and nanoparticles into YBCO thin films was reported in which BSO nanocolumns were combined with Y211 nanoparticles as hybrid APCs inside YBCO thin films by means of surface modified target method [52]. This new combination of hybrid APCs was also observed to be very effective in reducing the angular anisotropy of J_c of YBCO thin films. Figure 13 shows the cross-sectional micrograph of YBCO+Y211 and YBCO+BSO+Y211 thin films in which the formation of Y211 nanoparticles and that of BSO nanocolumns together with Y211 nanoparticles can be observed, respectively. The simultaneous incorporation of BSO nanocolumns and Y211 nanoparticles significantly improves the angular anisotropy of J_c in the hybrid APC sample which can be seen in figure 14. The thin film containing hybrid APCs exhibited the combined characteristics of nanoparticle pinning and nanocolumn pinning.

7. Factors determining the geometry/morphology of nanoscale inclusions:

Different secondary phase nanoinclusions inside YBCO film matrix exhibit different geometry and accordingly they are efficient for different range of applied magnetic field orientations. One of the fundamental parameters which decide the geometry of these nanoinclusions within YBCO film is the lattice misfit between the two phases. Another parameter which is important in determining the geometry of these nanoinclusions is the surface diffusion co-efficient of adatoms which is crucial in determining the interface between the two phases which may be coherent, semi-coherent or non-coherent [53]. While coherent and semi-coherent interfaces have much lower surface energies, that of the non-coherent interfaces are much higher which leads to coarsening of the grains in

polycrystalline films [54] and faceting of precipitates and grain boundaries [55]. In a recent work, it has been reported that the morphology of the secondary phase nanoinclusions is determined by the combined effect of the lattice mismatch and elastic properties of YBCO and secondary phase materials [56].

8. Conclusions

In order to improve the in-field J_c of YBCO superconducting thin films, many methods have been tried and introduction of APCs is crucial for this purpose. In recent years, a variety of methods have been reported to intentionally introduce nanostructured secondary phases into the YBCO superconducting thin films and among them, surface modified target method in PLD technique has been found to be very useful. Different secondary phases are formed in different geometries when incorporated within YBCO matrix and all these geometries can be realized by surface modified target method. The geometry and concentration of the secondary phase can be varied just by changing the composition and/or size of the secondary phase acting as surface modified piece on the ablation target. This is not only an economical approach but also saves a lot of time in conducting such experiments where the variation in the geometry and density of secondary phase material inside YBCO matrix is desired.

The generation of nanoscale secondary phases with desired density, geometry and orientation inside YBCO matrix is very much needed for control of vortex pinning in YBCO thin films deposited on single crystals and metallic tapes.

Acknowledgements

We thank T. Horide, S. Saini, P. Mele, A. Ichinose, Y. Yoshida and S. Awaji for cooperative research on vortex pinning studies in YBCO nanocomposite films.

References:

[1] M. K. Wu, J. R. Ashburn, C. J. Torng, P. H. Hor, R. L. Meng, L. Gao, Z. J. Huang, Y. Q. Wang and C. W. Chu, *Phys. Rev. Lett.* 58, 908 (1987).

[2] H. Maeda, Y. Tanaka, M. Fukutomi and T. Asano, *Jpn. J. Appl. Phys.* 27, L209 (1988).

[3] A. Schilling, M. Cantoni, J. D. Guo and H. R. Ott, *Nature* 363, 56 (1993).

[4] D. Larbalestier, A. Gurevich, D. M. Feldmann and A. Polyanskii, *Nature* 414, 368 (2001).

[5] A. P. Malozemoff, *Nat. Mater.* 6, 617 (2007).

[6] S. R. Foltyn, L. Civale, J. L. Macmanus-Driscoll, Q. X. Jia, B. Maiorov, H. Wang and M. Maley, *Nat. Mater.* 6, 631 (2007).

[7] K. Matsumoto and P. Mele, *Supercond. Sci. Technol.* 23, 014001 (2010).

[8] X. Obradors and T. Puig, *Supercond. Sci. Technol.* 27, 044003 (2014).

[9] D. Dimos, P. Chaudhari and J. Mannhart, *Phys. Rev. B* 41, 4038 (1990).

[10] S. Jin, T. H. Tiefel, R. C. Sherwood, R. B. van Dover, M. E. Davis, G. W. Kammlott, and R. A. Fastnacht, *Phys. Rev. B* 37, 7850 (1988).

[11] M. Murakami (Ed.), *Melt-processed High-Temperature Superconductors*, World Scientific, Singapore (1992).

[12] D. Dijkkamp, T. Venkatesan, X. D. Wu, S. A. Shaheen, N. Jisrawi, Y. H. Min-Lee, W. L. McLean and M. Croft, *Appl. Phys. Lett.* 51, 619 (1987).

[13] B. Schey, *Chapter 14 in "Pulsed Laser Deposition of Thin Films"*, by R. Eason (Ed.), Wiley, New Jersey, pp. 313–331 (2007).

[14] M. Miura, *Chapter 5 in "Oxide Thin Films, Multilayers, and Nanocomposites"*,

by P. Mele, T. Endo, S. Arisawa, C. Li and T. Tsuchiya (Eds.), Springer, Caham, Heidelberg, pp. 3–26 (2015).

[15] A. Ignatiev, *Chapter 15 in "Second-Generation HTS Conductors"*, by A. Goyal (Ed.), Kluwer Academic Publishers, Dordrecht, pp. 245–259 (2005).

[16] D. B. Chrisey, G.K. Hubler (Eds.), *Chapter 8 in "Pulsed Laser Deposition of Thin Films",* Wiley, New York, (1994).

[17] R. K. Singh, D. Kumar, *Mat. Sci. Eng. R*, 22, 113 (1998).

[18] T. Matsushita, *Chapter 1 in "Flux pinning in superconductors",* Springer, Berlin, Heidelberg, (2007).

[19] B. Dam, J. M. Huijbregtse, F. C. Klaassen, R. C. F. Van der Geest, G. Doornbos, J. H. Rector, A. M. Testa, S. Freisem, J. C. Martinez, B. Stauble-Pumpin and R. Griessen, *Nature* 399, 439 (1999).

[20] J. M. Huijbregtse, F. C. Klaassen, A. Szepielow, J. H. Rector, B. Dam, R. Griessen, B. J. Kooi and J. T. M. de Hosson, *Supercond. Sci. Technol.* 15, 395 (2002).

[21] L. Civale, *Supercond. Sci. Technol.* 10, A11 (1997).

[22] S. H. Wee, A. Goyal, P. M. Martin and L. Heatherly, *Supercond. Sci. Technol.* 19, 865 (2006).

[23] C. Cai, B. Holzapfel, J. Hanishch, L. Fernandez and L. Schultz, *Phys. Rev. B* 69, 104531 (2004).

[24] A. K. Jha, K. Matsumoto, T. Horide, S. Saini, P. Mele, A. Ichinose, Y. Yoshida, and S. Awaji, *J. Appl. Phys.* 122, 093905 (2017).

[25] T. Haugan, P. N. Barnes, R. Wheeler, F. Meisenkothen and M. Sumption, *Nature*

430, 867 (2004).

[26] A. A. Gapud, D. Kumar, S. K. Viswanathan, C. Cantoni, M. Varela, J. Abiade, S. J. Pennycook and D. K. Christen, *Supercond. Sci. Technol.* 18, 1502 (2005).

[27] J. L. MacManus Driscoll, S. R. Foltyn, Q. X. Jia, H. Wang, A. Serquis, L. Civale, B. Maiorov, M. E. Hawley, M. P. Maley and D. E. Peterson, *Nat. Mater.* 3, 439 (2004).

[28] A. Goyal, S. Kang, K. J. Leonard, P. M. Martin, A. A. Gapud, M. Varela, M. Paranthaman, A. O . Ijaduola, E. D. Specht, J. R. Thompson, D. K. Christen, S. J. Pennycook and F. A. List, *Supercond. Sci. Technol.* 18, 1533 (2005).

[29] P. Mele, K. Matsumoto, A. Ichinose, M. Mukaida, Y. Yoshida, S. Horii and R. Kita, *Supercond. Sci. Technol.* 21, 125017 (2008).

[30] C. V. Varanasi, J. Burke, H. Wang, J. H. Lee and P. N. Barnes, *Appl. Phys. Lett.* 93, 092501 (2008).

[31] J. Hanisch, C. Cai, R. Huhne, L. Schultz and B. Holzapfel, *Appl. Phys. Lett.* 86, 122508 (2005).

[32] D. M. Feldmann, T. G. Holesinger, B. Maiorov, S. R. Foltyn, J. Y. Coulter and I. Apodaca, *Supercond. Sci. Technol.* 23, 095004 (2010).

[33] S. H. Wee, A. Goyal, Y. L. Zuev, C. Cantoni, V. Selvamanickam and E. D. Specht, *Appl. Phys. Exp.* 3, 023101 (2010).

[34] S. H. Wee, A. Goyal, E. D. Specht, C. Cantoni, Y. L. Zuev, V. Selvamanickam and S. Cook, *Phys. Rev. B* 81, 140503 (2010).

[35] C. Varanasi, P. N. Barnes, J. Burke, J. Carpenter and T. Haugan, *Appl. Phys. Lett.* 87, 262510 (2005).

[36] P. Mele, K. Matsumoto, T. Horide, A. Ichinose, M. Mukaida, Y. Yoshida and S. Horii, *Supercond. Sci. Technol.* 20, 616 (2007).

[37] P. Mele, K. Matsumoto, T. Horide, A. Ichinose, M. Mukaida, Y. Yoshida and S. Horii, *Supercond. Sci. Technol.* 20, 244 (2007).

[38] T. Horide, K. Matsumoto, A. Ichinose, M. Mukaida, Y. Yoshida and S. Horii, *Supercond. Sci. Technol.* 20, 303 (2007).

[39] M. Tachiki and S. Takahashi, Sol. St. Comm. 70, 291 (1989).

[40] M. Tachiki and S. Takahashi, Sol. St. Comm. 72, 1083 (1989).

[41] L. Civale, B. Maiorov, A. Serquis, J. O. Willis, J. Y. Coulter, H. Wang, Q. X. Jia, P. N. Arendt, J. L. MacManus Driscoll, M. P. Maley, and S. R. Foltyn, *Appl. Phys. Lett.* 84, 2121 (2004).

[42] S. K. Viswanathan, A. A. Gapud, M. Varela, J. T. Abiade, D. K. Christen, S. J. Pennycook and D. Kumar, Thin Solid Films, 515, 6452 (2007).

[43] P. Mele, R. Guzman, J. Gazquez, T. Puig, X. Obradors, S. Saini, Y. Yoshida, M. Mukaida, A. Ichinose, K. Matsumoto and M. I. Adam, *Supercond. Sci. Technol.* 28, 024002 (2015).

[44] C. V. Varanasi, P. N. Barnes, J. Burke, L. Brunke, I. Maartense, T. J. Haugan , E. A. Stinzianni, K. A. Dunn and P. Haldar, *Supercond. Sci. Technol.* 19, L37 (2006).

[45] C. V. Varanasi, J. Burke, L. Brunke, H. Wang, M. Sumption and P. N. Barnes, *J. Appl. Phys.* 102, 063909 (2007).

[46] P. Mele, K. Matsumoto, T. Horide, A. Ichinose, M. Mukaida, Y. Yoshida and S. Horii, *Physica C*, 463-465, 653 (2007).

[47] A. K. Jha, K. Matsumoto, T. Horide, S. Saini, P. Mele, Y. Yoshida and S. Awaji, *Supercond. Sci. Technol.* 27, 025009 (2014).

[48] P. Mele, K. Matsumoto, T. Horide, A. Ichinose, M. Mukaida, Y. Yoshida, S. Horii and R. Kita *Physica C* 468, 1631 (2008).

[49] P. Mele, K. Matsumoto, T. Horide, A. Ichinose, M. Mukaida, Y. Yoshida, S. Horii and R. Kita, *Supercond. Sci. Technol.* 21, 015019 (2008).

[50] A. K. Jha, K. Matsumoto, T. Horide, S. Saini, P. Mele, Y. Yoshida and S. Awaji, *IEEE Trans. Appl. Supercond.* 25, 8000505 (2015).

[51] A. K. Jha, K. Matsumoto, T. Horide, S. Saini, P. Mele, A. Ichinose, Y. Yoshida and S. Awaji, *Supercond. Sci. Technol.* 28, 114004 (2015).

[52] A. K. Jha, K. Matsumoto, T. Horide, S. Saini, P. Mele, A. Ichinose, Y. Yoshida and S. Awaji, *IEEE Trans. Appl. Supercond.* 26, 2525989 (2016).

[53] J. Gutierrez, A. Llordes, J. Gazquez, M. Gibert, N. Roma, S. Ricart, A. Pomar, F. Sandiumenge, N. Mestres, T. Puig and X. Obradors, *Nat. Mater.* 6, 367 (2007).

[54] C. V. Thomson, *Annu. Rev. Mater. Sci.* 30, 159–190 (2000).

[55] A. Sutton and R. Balluffi, *Interfaces in Crystalline Materials, Oxford Univ. Press, Oxford* (1996).

[56] J. Wu and J. Shi, *Supercond. Sci. Technol.* 30, 103002 (2017).

Figures

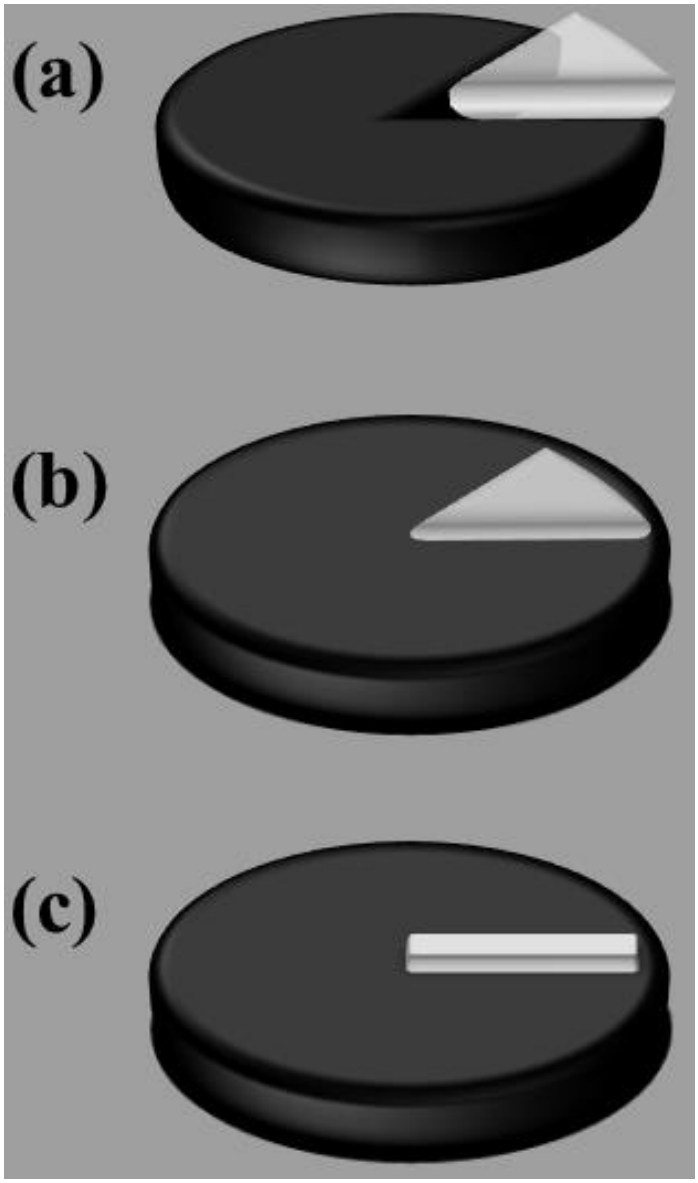

Fig. 1 Schematic diagram of the ablation target used in surface modified target method. (a) Ideally, it is desired to cut a sectoral slot where a wedge shaped secondary phase piece can be inserted. (b) Instead, a thin sectored slice of secondary phase materials is attached to the top surface of the YBCO target. (c) The secondary phase slice can also be made in rectangular form which can be attached to the top surface of YBCO target by means of silver paste.

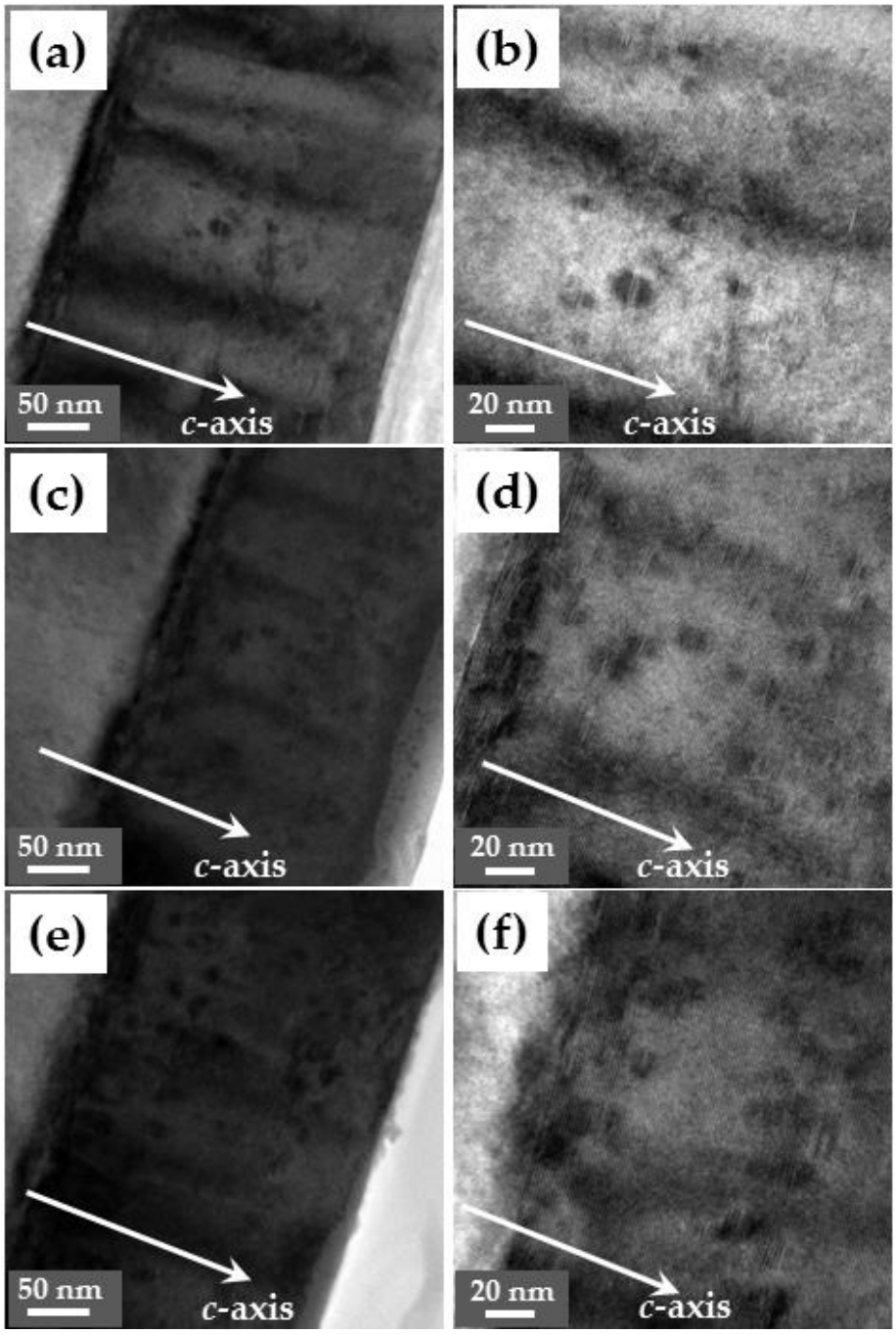

Fig. 2 The cross-sectional TEM image of YBCO+Y211 nanocomposite films prepared using surface modified target method with varying concentration of Y211 nanoparticles at two different magnifications. (a) and (b) represent least concentration of Y211 nanoparticles, (c) and (d) represent medium concentration and (e) and (f) represent maximum concentration. Reprinted from [24], with the permission of AIP Publishing.

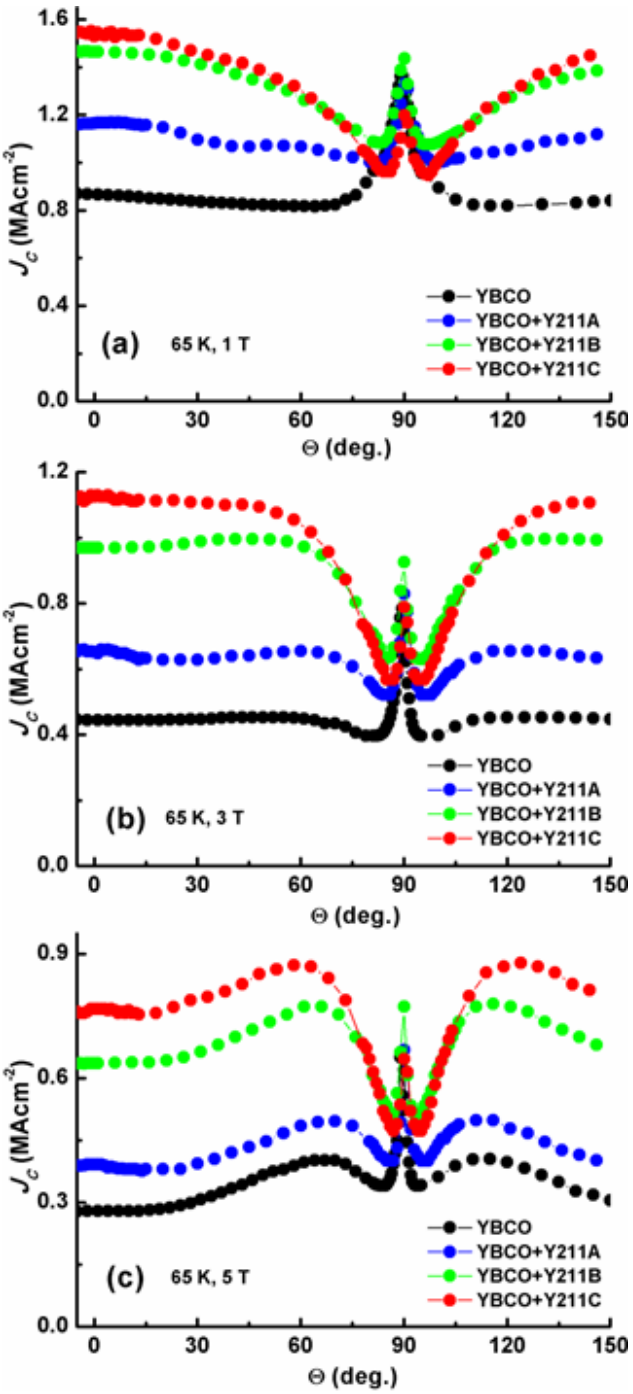

Fig. 3 Variation of J_c with the orientation the applied magnetic field for pristine YBCO and YBCO+Y211 films with varying concentrations of Y211 nanoparticles measured at 1, 3 and 5 T at 65 K. The isotropic enhancement in J_c of YBCO+Y211 films can be clearly observed at all the magnetic fields. Reprinted from [24], with the permission of AIP Publishing.

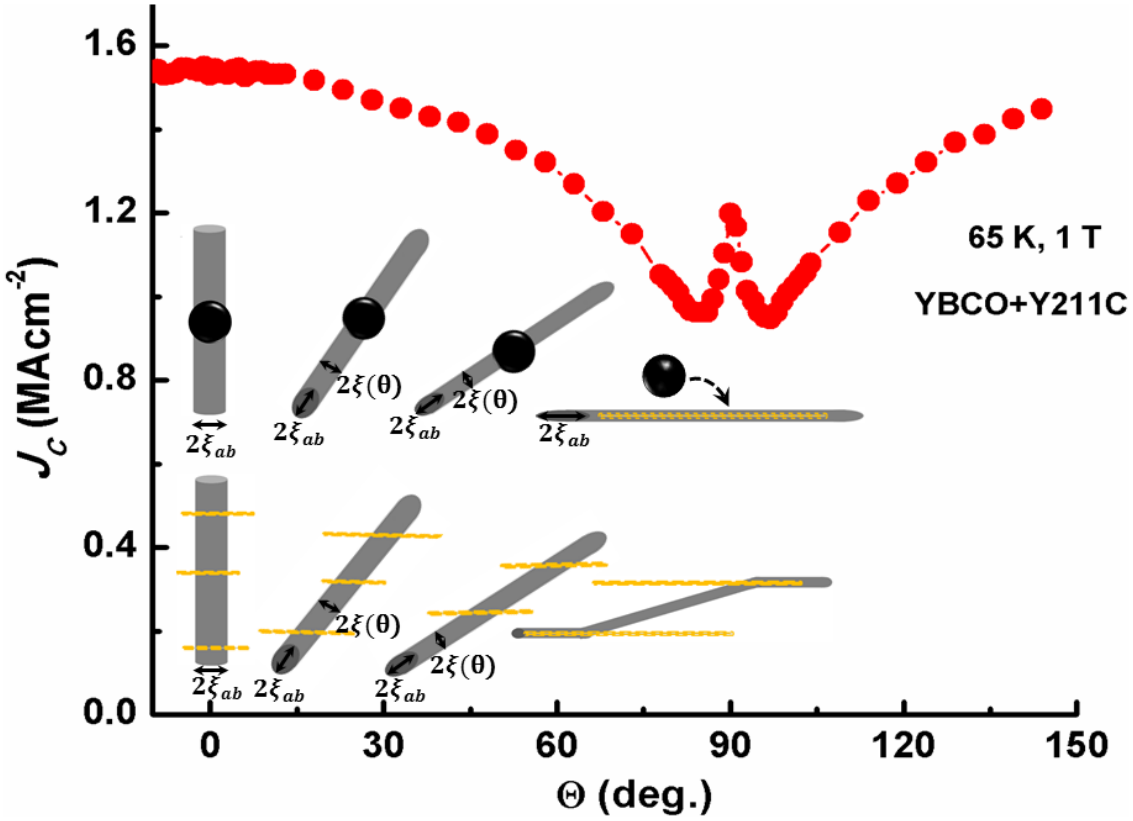

Fig. 4 Schematic diagram of dominating angular regime of pinning for Y211 nanoparticles and planar defects. As the vortices are inclined from the *c*-axis, the interaction volume with the spherical defects decreases and the pinning energy is decreased resulting in overall decrease in J_c. Planar defects along the *ab*-plane, can pin the vortices only for limited angular regime and act as linear defects with small accommodation angle. Reprinted from [24], with the permission of AIP Publishing.

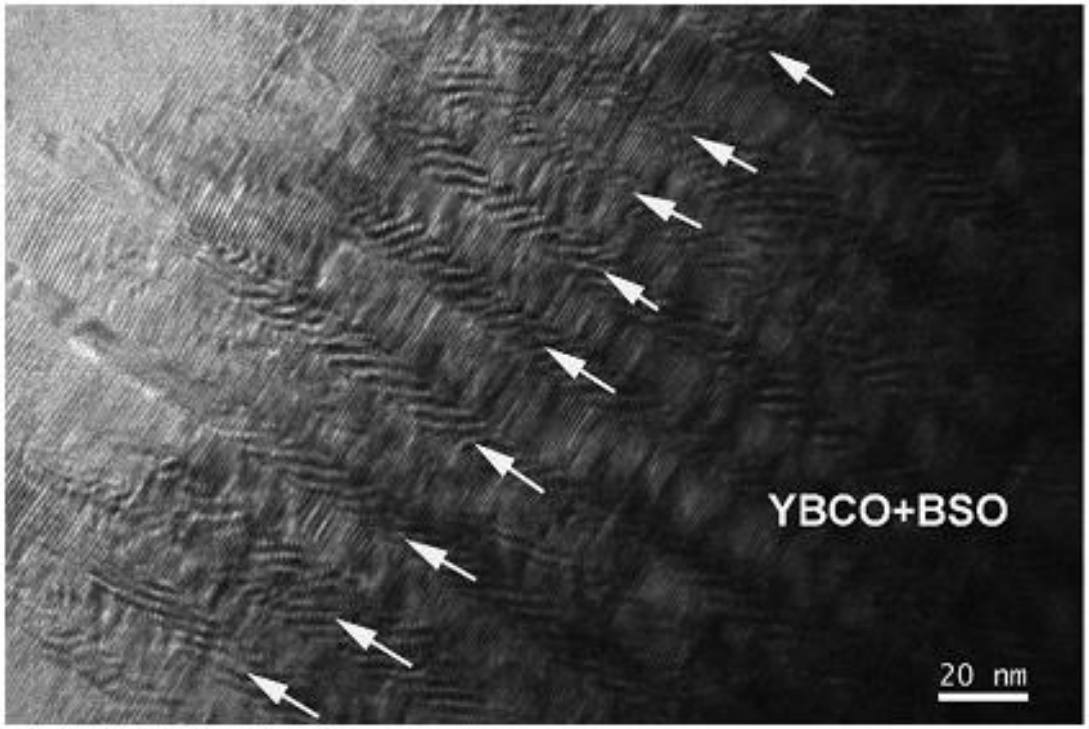

Fig. 5 Cross-sectional TEM image of YBCO film with BSO nanoinclusions deposited by surface modified target method using PLD technique. The image shows that BSO nanostructures are self-assembled in the form of nanocolumns aligned along the crystallographic *c*-direction. Reprinted from [30], with the permission of AIP Publishing.

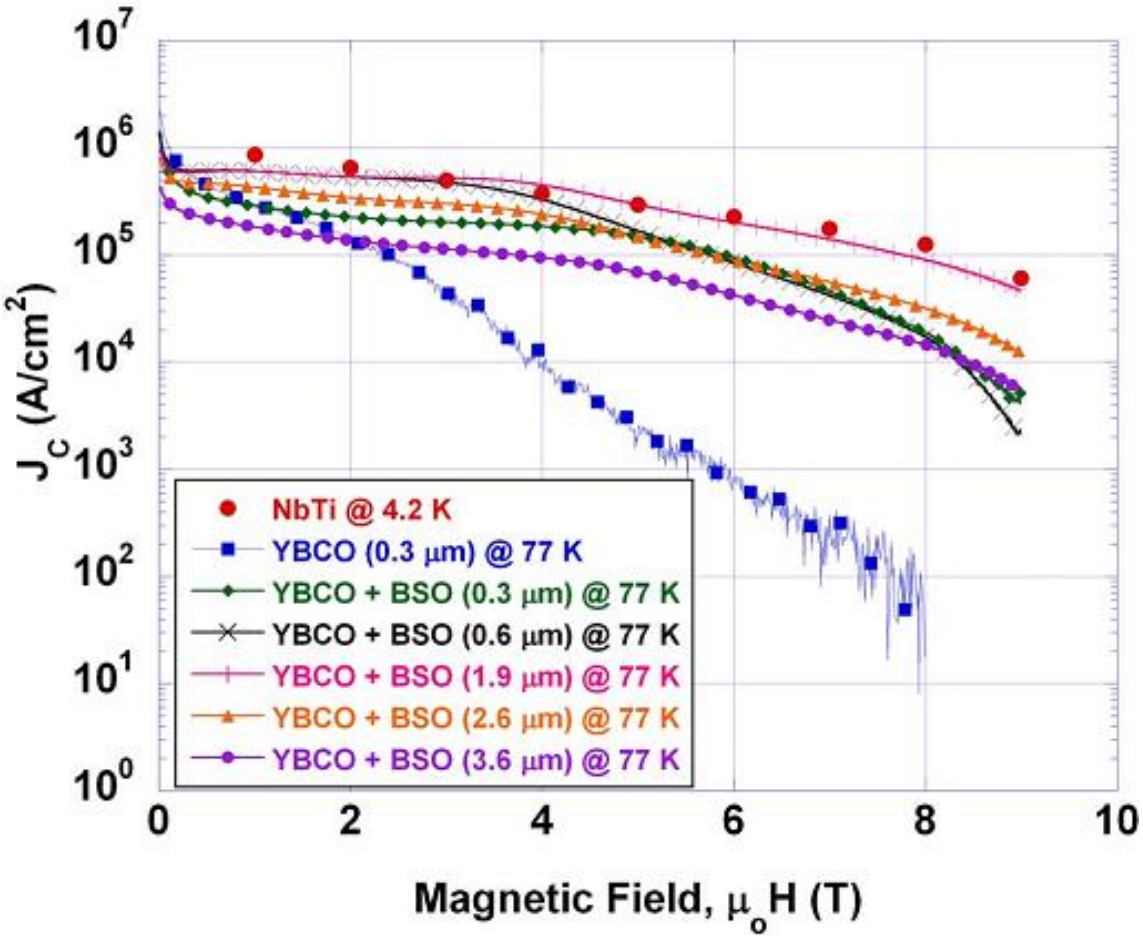

Fig. 6 Variation of J_c with applied magnetic field for pristine YBCO film and YBCO films with BSO nanoinclusions with varying thickness. The enhanced in-field J_c can be clearly observed in YBCO films incorporating BSO nanoinclusions. Reprinted from [30], with the permission of AIP Publishing.

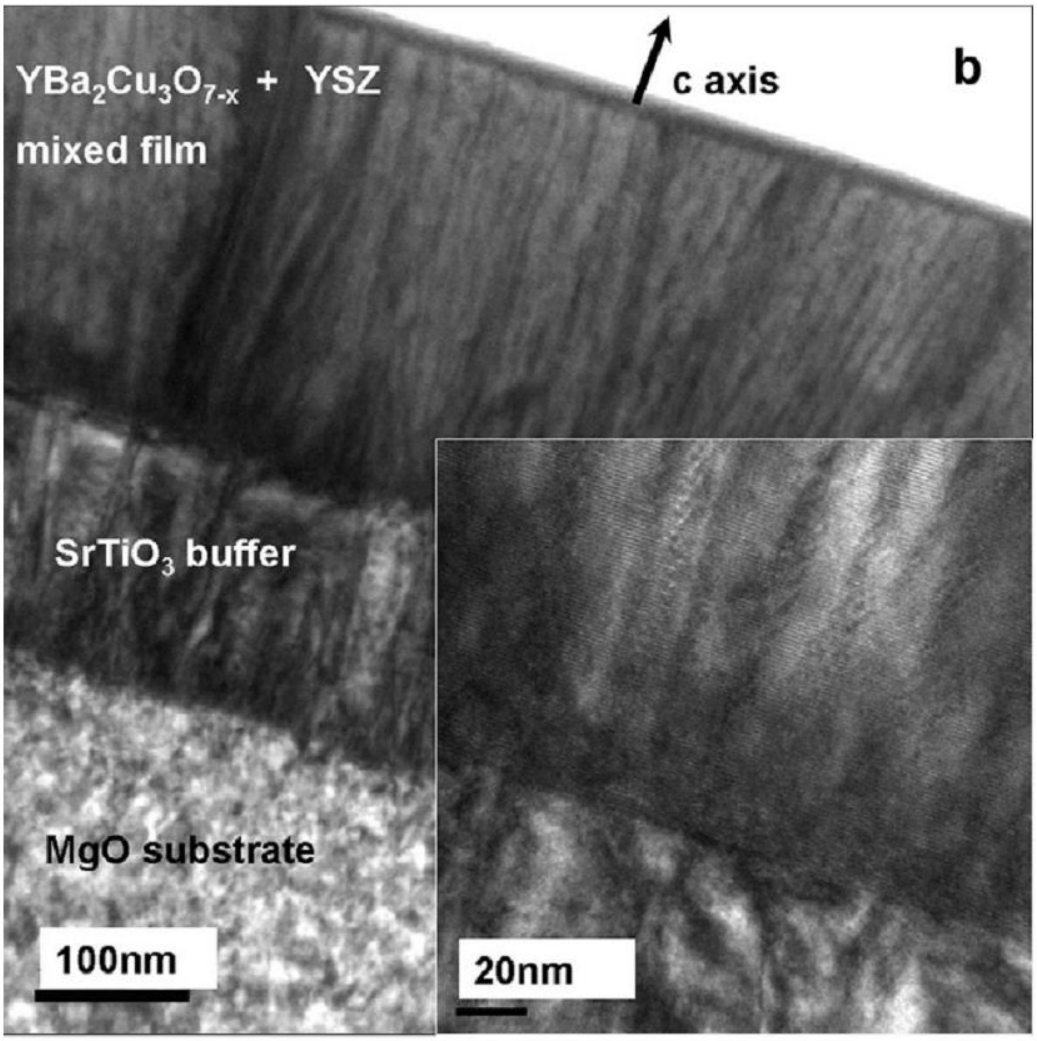

Fig. 7 Cross-sectional TEM image of YBCO+YSZ film deposited by surface modified target method using PLD technique. The formation of BZO nanorods can be seen clearly which were later confirmed by XRD measurement. Reprinted from [46], with the permission of Elsevier.

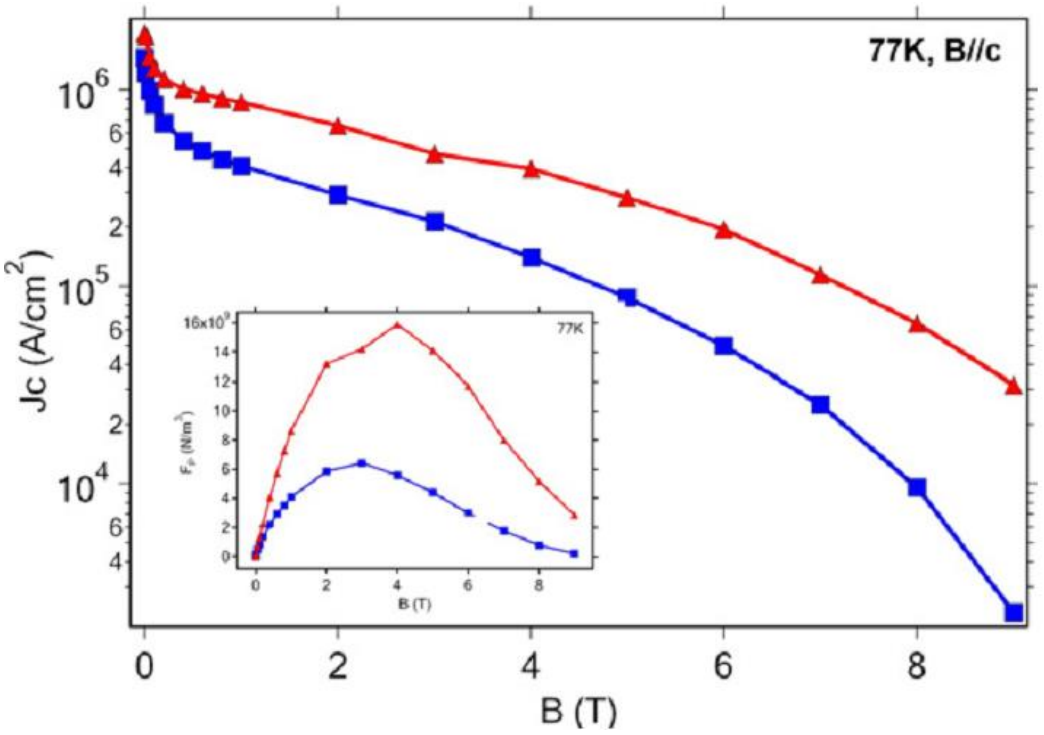

Fig. 8 Variation of J_c with respect to applied magnetic field for pristine YBCO (blue) and YBCO+YSZ (red) films prepared using surface modified target method. Inset shows the variation of F_p with applied magnetic field in which much higher F_{pmax} for the nanocomposite films can be observed. Reprinted from [46], with the permission of Elsevier.

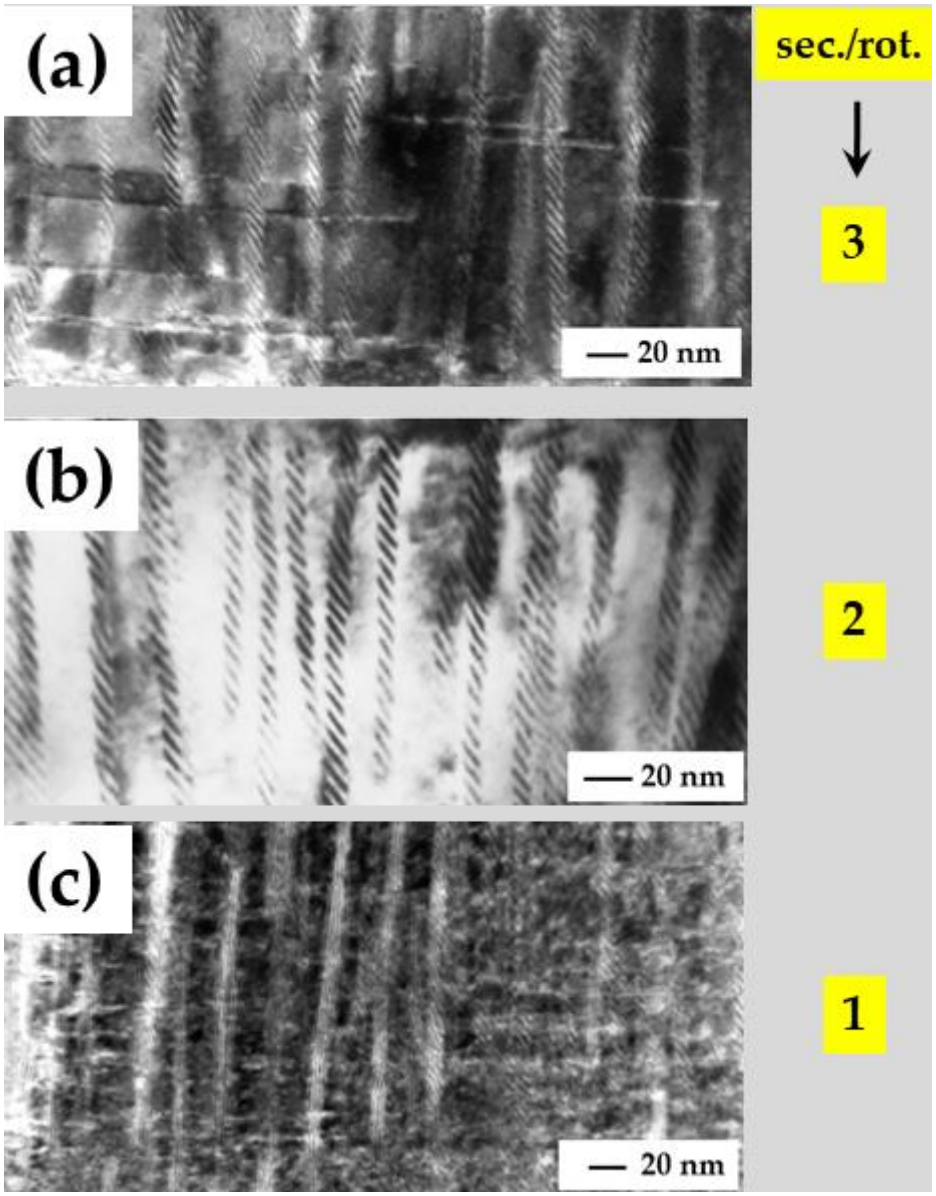

Fig. 9 Cross-sectional TEM image of YBCO film with YBNO nanocolumns prepared using surface modified target method. The density of the YBNO columns was varied by controlling the target rotation speed in the PLD system.

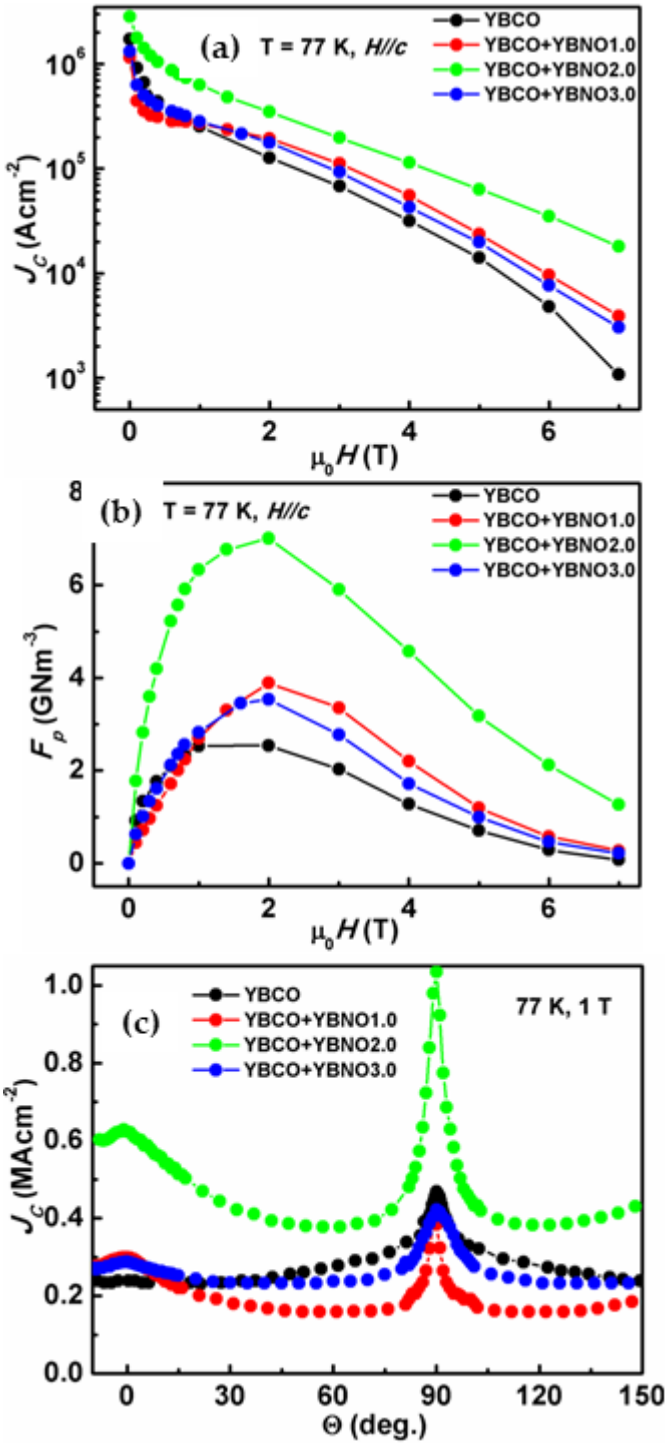

Fig. 10: Variation of (a) J_c and (b) F_p with respect to applied magnetic field for YBCO films with varying concentration of YBNO nanocolumns. YBCO+YBNO films exhibit superior in-field J_c as compared to pristine YBCO film. (c) Angular dependent J_c measurement shows that YBCO+YBNO films exhibit a J_c peak near 0 deg. (*H//c*-axis).

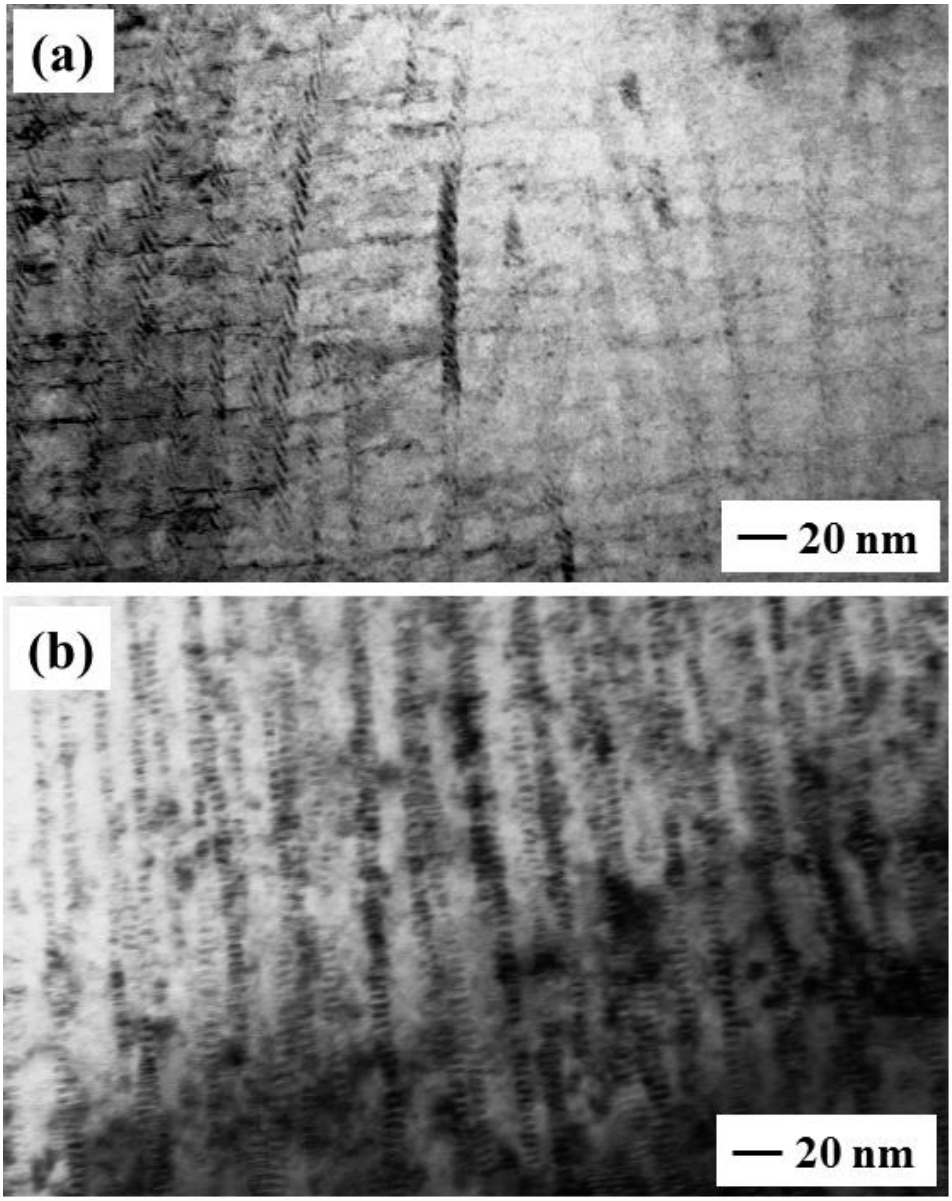

Fig. 11 Cross-sectional TEM image of YBCO films with (a)BSO nanocolumns and (b) BSO nanocolumns and Y_2O_3 nanoparticles deposited by surface modified target method. Reproduced from ref. [50], with the permission from IEEE Publishing.

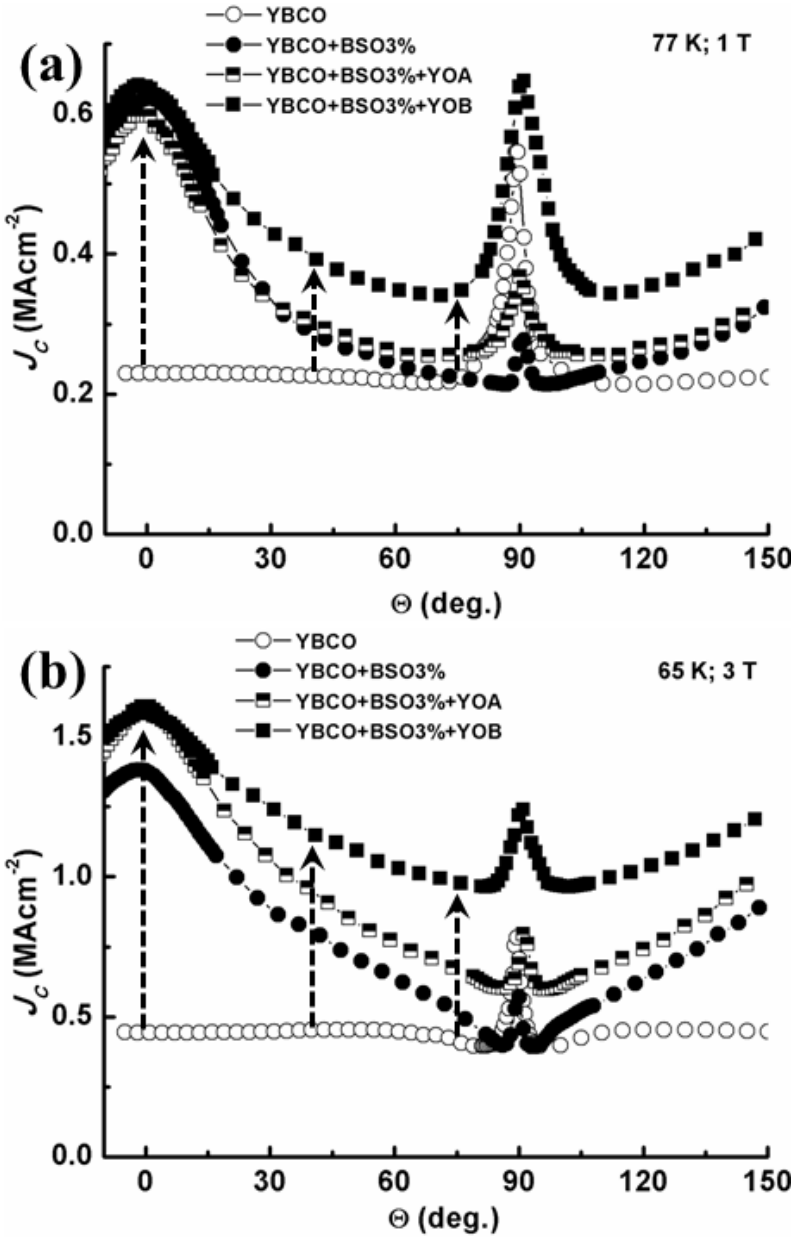

Fig. 12 Angular dependent J_c characteristics of pristine YBCO, YBCO+BSO, and YBCO+BSO+Y_2O_3 nanocomposite films measured at (a) 77 K, 1 T and (b) 65 K, 3 T. Two different sizes of sectored Y_2O_3 pieces, 2.2 area% and 3 area%, are referred as YOA and YOB, respectively. Reproduced from ref. [50], with the permission from IEEE Publishing.

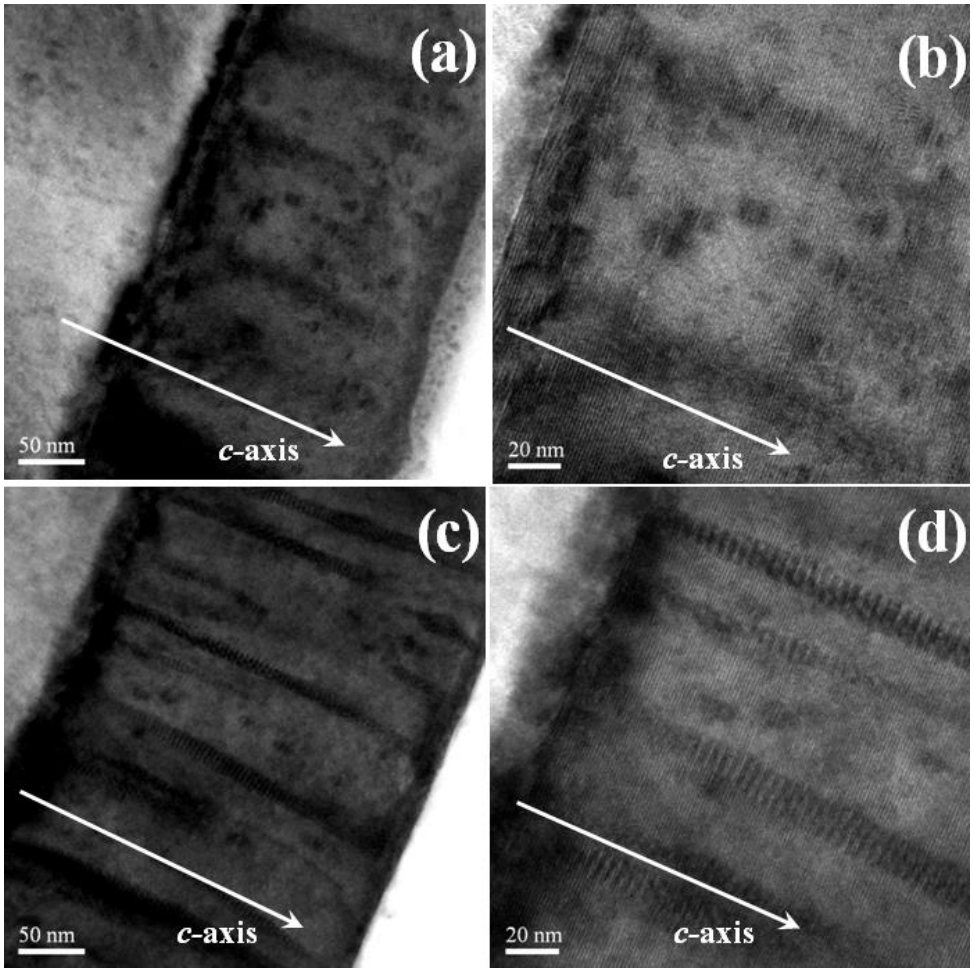

Fig. 13 Cross-sectional TEM image of YBCO thin films with Y211 nanoparticles (a) and (b) and BSO nanocolumns plus Y211 nanoparticles (c) and (d) deposited by surface modified target method. Reproduced from ref. [52], with the permission from IEEE Publishing.

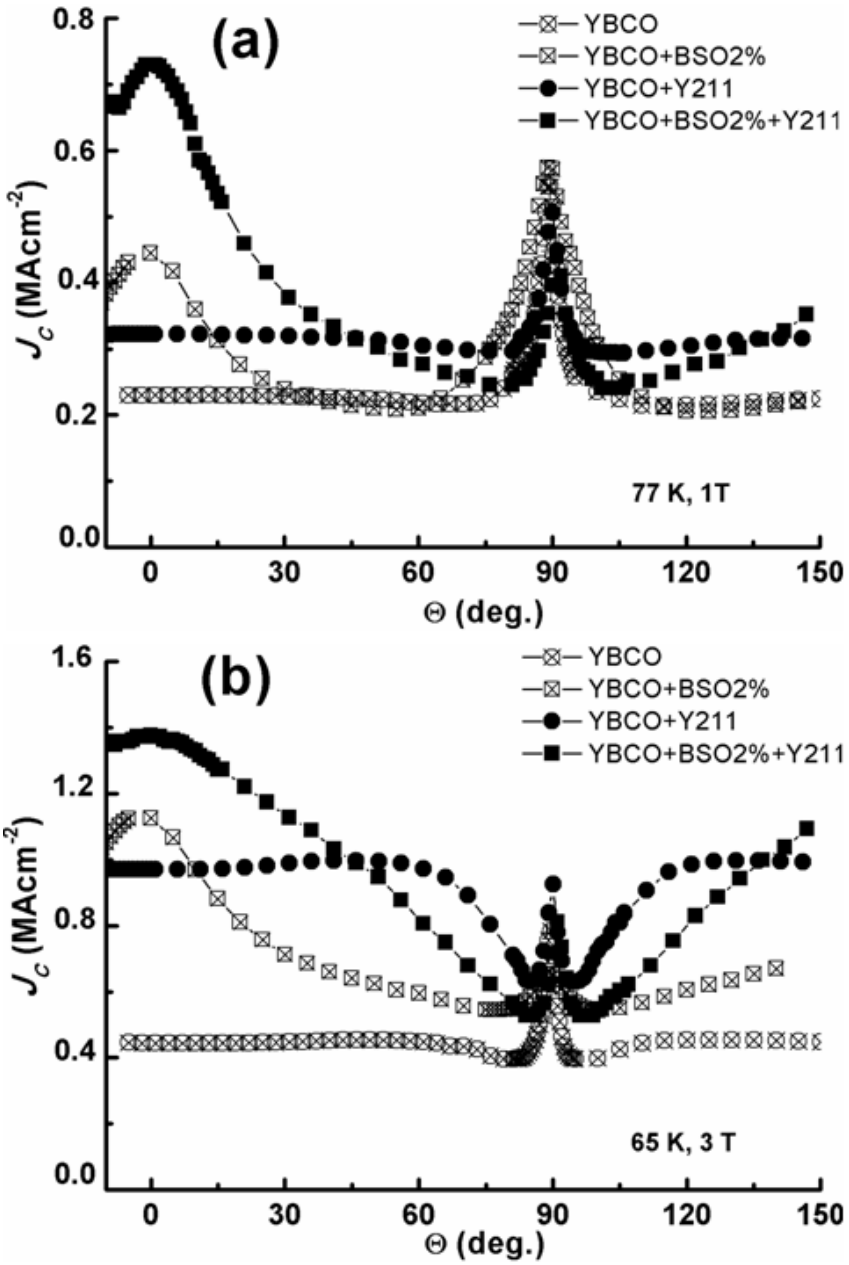

Fig. 14 Angular dependent J_c characteristics of pristine YBCO, YBCO+BSO, YBCO+Y211 and YBCO+BSO+Y211 nanocomposite thin films measured at (a) 77 K, 1 T and (b) 65 K, 3 T. Reproduced from ref. [52], with the permission from IEEE Publishing.